FTIR *in situ* measurement of swelling and CO_2 sorption in acrylic polymers at high CO_2 pressures

Margaux Haurat[1] (corresponding author at : margaux.haurat@u-bordeaux.fr), Thierry Tassaing[2], Michel Dumon[1]

[1] Univ. Bordeaux, CNRS, Bordeaux INP, LCPO, UMR 5629, F-33600 Pessac, France

[2] Institut des Sciences Moléculaires, Université de Bordeaux, UMR 5255 CNRS, 351 Cours de la Libération, F-33405, Talence Cedex, France

Keywords: FTIR microscopy, CO_2 foaming, PMMA, MAM, CO_2 sorption, swelling

Abstract

A FTIR (Fourier Transform Infrared) microscope combined to a CO_2 high-pressure cell has been used to determine simultaneously the CO_2 uptake and the swelling of several acrylic polymer systems, precursors of CO_2-foamed polymers (PMMA), a triblock copolymer (MAM) and a PMMA/10 wt% MAM blend. Samples were isothermally saturated with supercritical CO_2 ($scCO_2$) up to high- CO_2 pressures (5, 10, 30 MPa) at 40 °C and 130 °C. The behavior upon pressure increase is indeed different at the two temperatures in the three systems, showing either a linear or a plateau shape. These two types of regimes are analyzed in view of literature. Addition of 10 wt% MAM copolymer led to a significant increase of CO_2 uptake (23 % for neat PMMA to 42 % for the blend, 40 °C, 30 MPa). Such data are useful to further find out the best routes to produce low-density and nanoporous polymer foams, using $scCO_2$ as foaming agent.

1. Introduction

In the large field of porous materials, foams have been fabricated for a long time following various methods, either chemical [1],[2], or physical [3],[4],[5]. On the one hand, chemical foaming requires the use of chemical blowing agents (CBA). Once thermally degraded or thanks to a chemical reaction, this agent generates a gas responsible of the so-called chemical foaming. On the other hand, it is possible to directly inject a gas (or a supercritical fluid) in a process to create porosities by gas expansion during the depressurization. For a few years, this solution (physical foaming) has been largely studied in order to replace some traditional CBA that tend to be forbidden by REACH regulation (e.g. azodicarbonamide).

Supercritical carbon dioxide ($scCO_2$) has been mostly used as an available, cheap and non-toxic physical foaming agent in many polymers [6],[7],[8],[9]. Moreover, its critical point is rather "low" (31 °C and 7.4 MPa) so it is quite easy to reach the CO_2 critical state and take advantage of the combination of gaseous and liquid properties: good diffusivity and a good solvent capability [10],[11].

In order to evaluate the foamability of a polymer (or a polymer blend) in presence of $scCO_2$ different parameters have to be evidenced : the CO_2 ability to diffuse in and out of the polymer under supercritical conditions, sorption, desorption and polymer swelling (dilatation). In this article, we will both focus on CO_2 sorption and polymer (and blends) swelling during the saturation step before foaming.

CO_2 sorption into polymers can be characterized by various methods or devices : gravimetric method [12],[13], quartz microbalance (QCM) [14],[15],[16] or magnetic suspension balance (MSB) [17],[18]. All of them consist in calculating the mass variation before and after CO_2 saturation but the fast desorption of the sample induces some errors on the % mass CO_2 determination.

This CO_2 uptake can also be determined with spectra recorded thanks to Fourier transform infrared (FTIR) microscopy [11],[19],[20],[21],[22]. As shown in this study, the use of a FTIR microscope set-up with a high-pressure cell, is a way to simultaneously measure swelling and CO_2

sorption at high pressures and at the desired temperatures. This *in situ* method provides information about the behavior of the studied materials facing the CO_2 saturation, under given conditions (P, T) selected to mimic CO_2 saturation in a foaming process. For example, in a batch process ("solid state foaming", represented by a typical temperature of 40 °C) or a continuous process ("melt foaming", represented by a typical temperature of 130 °C) - e.g. CO_2 extrusion -, foaming requires to optimize $scCO_2$ saturation at several pressures. In this study, swelling and CO_2 sorption with increasing P and T of acrylic polymer systems are studied inside the spectroscopic cell, mimicking different processes saturating conditions.

The final goal is to produce "nanofoams" by a continuous process namely extrusion foaming. In acrylic systems CO_2 assisted extrusion (130 °C and 10 to 30 MPa) [23],[24] generally leads (at the best) to micro cellular foams; whereas following a discontinuous process (batch foaming) in the same pressure range but considerably lower temperatures (around 40 °C), it is proved to be easier to obtain acrylic quasi nano foams [3]. Our study should help enhancing and optimizing conditions of nano foaming. Foams, when reducing both cell size and density at the same time, are intended to exhibit enhancement of several properties, such as high thermal insulation [25] or high performance mechanical properties [26] (damping) or else useful for filtration [13].

The material's choice is focused on an acrylic blend containing 90 wt% of poly(methyl methacrylate), PMMA and 10 wt% of a triblock copolymer poly(methyl methacrylate)-co-poly(butyl acrylate)-co- poly(methyl methacrylate), MAM (i.e. PMMA-PBA-PMMA, PBA is poly(butyl acrylate)). This additive is more CO_2-philic than PMMA thanks to the butyl acrylate center block [27],[28],[29]. The neat PMMA matrix and neat MAM copolymer are also studied separately. Generally in the field of polymer foams, these three acrylic polymers are considered as good CO_2-foamable candidates due to their good affinity with CO_2 (thanks to the presence of the carbonyl groups), in comparison with other kind of polymers [9].

Thus the present paper quantifies CO_2 sorption, swelling and identifies the trends when temperature and/or pressure increase ; especially in view of optimizing the CO_2 uptake in a short time, while maximizing expansion and controlling a high cell density.

2. Materials and Methods

2.1. Materials

Carbon dioxide N45 (purity 99 %) was supplied by Air Liquide. Pellets of poly(methyl methacrylate) (PMMA) and MAM (poly(methyl methacrylate)-co-poly(butyl acrylate)-co- poly(methyl methacrylate) triblock copolymer were kindly supplied by Arkema (Lacq, France). Details on the initial materials can be found in literature [27],[28],[30][4] and are summarized in Table 1.

For the preparation of the PMMA/10 wt% MAM blend, PMMA and MAM pellets, were first dried 4 h at 80 °C. Then the blend was compounded by CANOE (Pau, France) using a corotative twin screw extruder (Labtech $\emptyset = 26\ mm,\ {}^{L}/_{D} = 40$) with a temperature profile ranging from 250 to 230 °C at a screw speed of 300 rpm. Then, the blends were pelletized using a continuous cutting machine operating at the end of the line.

The PMMA, MAM and PMMA/10 wt% MAM thin films ($e \approx 0.5\ mm; L \approx 4\ mm; l \approx 1\ mm$) were made by dissolving pellets in tetrahydrofuran solvent (THF) at 60 °C and evaporated overnight at 85 to 90 °C.

Table 1: Characteristics of the polymers used

Material	State at room temperature	M_n (g.mol^{-1})	M_w (g.mol^{-1})	Other characteristics	Density (g.cm^{-3})	Aspect
PMMA V825T clear 101	glassy amorphous solid	43 000	83 000	use as polymer matrix	1.19	transparent
	rubbery center	82 000	128 000	used as an additive	1.03*	transparent

MAM M53	block + glassy end-blocks	triblock copolymer PMMA-PBA-PMMA 54 wt% PBA

* measured with a water pycnometer

2.2. Infrared micro-spectroscopy

2.2.1. Experimental set-up (device, P, T, cell)

A FTIR microscope (Perkin Elmer Spotlight 200) working in transflection mode was used to record infrared spectra of the studied materials. With this set-up it is possible to investigate the spectral range from 800 to 6500 cm^{-1} with a spatial resolution of 100 µm. Thanks to the microscope linked to the FTIR set-up, one can precisely focus the FTIR beam on the a specific part of the high-pressure cell (either in the sample or on a mirror as shown in Figure 1).

In order to maintain the sample in an area saturated with CO_2 at high pressure, it was placed between a mirror and a sapphire window constituting the high-pressure cell as shown in Figure 1.

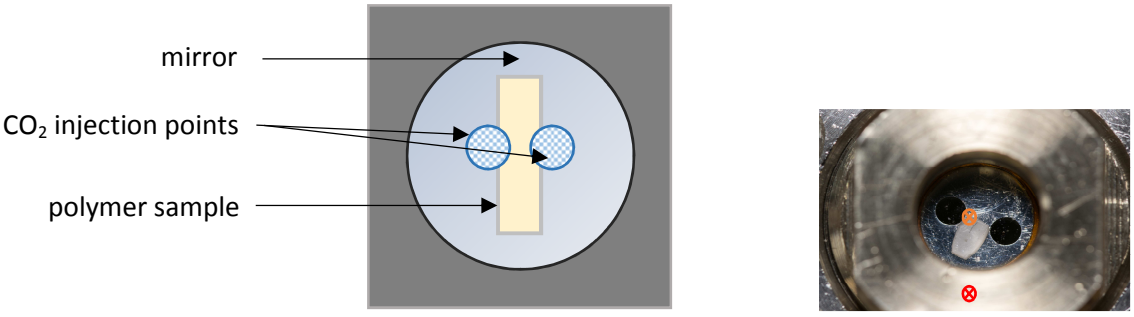

Figure 1: FTIR CO_2 high-pressure cell used to measure the polymer absorbance (red arrow location) or the CO_2 absorbance (orange arrow location); a) scheme of top view, b) photograph of a sample inside the high-pressure cell

This cell was CO_2 powered at the desired pressure (up to 40 MPa) thanks to a stainless-steel capillary linked to a hydraulic pressurizing system. The temperature in the cell was regulated thanks to 4 cartridge heaters distributed all around the cell and was measured with 2 thermocouples respectively located close to the sample area and close to a cartridge heater (Figure 2). For each

pressure or temperature modification, a stabilization time was necessary and evaluated by recording several consecutive spectra.

In this study the experiments were conducted at 40 °C or 130 °C and in a pressure range from 5 MPa to 30 MPa.

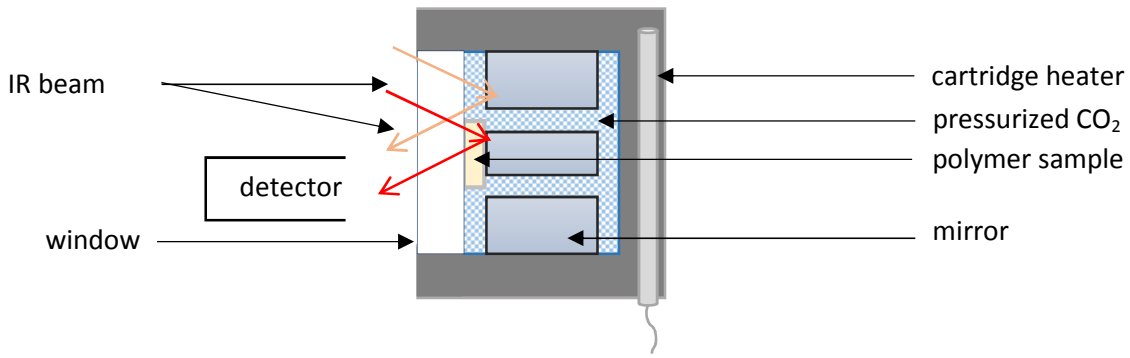

Figure 2: Experimental FTIR set-up

2.2.2. Experimental procedure

As shown in Figure 1, the thin polymer sample (about 0.5 mm) was centered between the two CO_2 arrivals before being fixed between a stainless-steel polished mirror and the window of the cell. Under these conditions, the CO_2 can diffuse inside the cell and saturate the studied sample. Samples are allowed to swell on their non-constrained edges. Although in a batch configuration the swelling is possible in all 3 dimensions (3D), we emphasize that the polymers under investigation are isotropic in nature and we do not expect to have any influence on the swelling of the polymer even if the polymer can swell in only 2 dimensions in our IR microscopy configuration. This expected behavior was checked by Champeau et al. [21] on swelling and CO_2 sorption measurement in Polyethylene Oxide (PEO). The results obtained using a 2D configuration with Infrared microscopy were in a good agreement with literature data that were obtained under experimental conditions where the polymer could swell in 3D configuration. Finally, some of the results obtained in this study

are found to be in a rather good agreement with literature data obtained in 3D configuration. The discrepancies observed between the different set of data are mainly due to the experimental errors that are inherent to the different methods used in the literature.

After sample positioning, the cell was heated up to the chosen temperature (40 °C or 130 °C). Once the temperature was reached, a first spectrum was recorded without CO_2 (red location shown in Figure 1). Then, CO_2 was injected at the desired pressure (5 – 10 – 20 – 30 MPa). During the pressure stabilization a spectrum was recorded every 5 min to follow the CO_2 sorption in the material over time.

In this study, the equilibrium was generally reached after 30 to 90 min. At the end of the experiment, samples were taken out of the cell as transparent pieces (unfoamed) or slightly white pieces (close to the beginning of foaming when the cell was quickly depressurized).

2.3. Infrared spectra and data analysis

2.3.1. Near-infrared absorption spectra (i.e. 6500 – 2000 cm^{-1})

For each sample, the infrared spectrum of the polymer or blend swelled by CO_2 was recorded at 40 °C and at 130 °C for pressures ranging between 5 and 30 MPa.

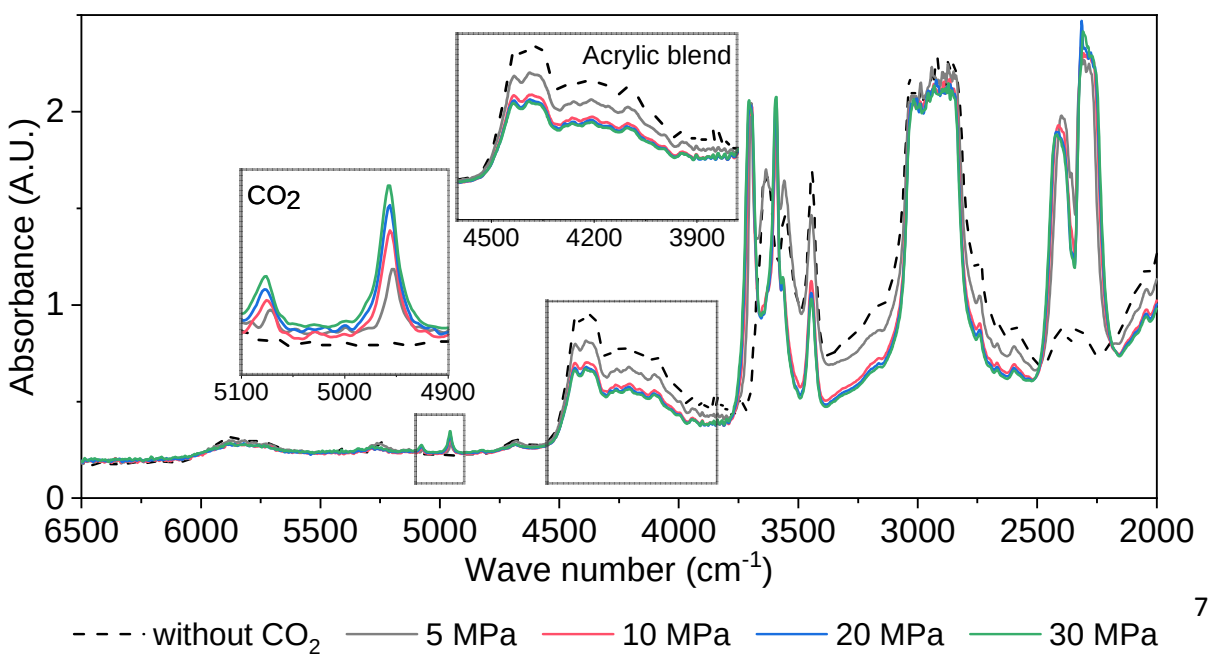

Figure 3: Infrared spectra of MAM at 40 °C without CO_2 and with CO_2 at P = 5-10-20-30 MPa, showing the spectral regions used for quantitative analysis

As shown in Figure 3, the CO_2 addition leads to spectra modifications. Different peaks associated with fundamental and combination modes of CO_2 can be observed at different wavenumbers (see Table 2). In order to determine the CO_2 mass uptake and swelling of our polymers and blend both CO_2 and polymers peaks were studied.

Table 2: IR spectral contributions of CO_2 in the spectral range 2000-5100 cm^{-1} [11]

Peak wavenumber (cm^{-1})	**CO_2 contribution**
2350	ν_3
3590	$2\nu_2 + \nu_3$
3695	$\nu_1 + \nu_3$
4950	$\nu_1 + 2\nu_2 + \nu_3$
5030	$2\nu_1 + \nu_3$
4850	$4\nu_2 + \nu_3$

ν_1 : symmetric stretching mode; ν_2 : CO_2 bending mode; ν_3 : antisymmetric stretching mode

For a quantitative analysis, we have selected non saturated (to avoid neither a too large absorbance, e.g. A > 1, nor too weak absorbance, e.g. A < 0.1) significant peaks associated with the polymer and the sorbed CO_2 at both 40 °C and 130 °C over a pressure range from 5 to 30 MPa. Then, these peaks were integrated from different onsets and endsets, and several areas were calculated (more details in Supporting Information). Finally, each set of values was used for the calculation of the CO_2 sorption, C_{CO_2} (mol.L^{-1}), the CO_2 mass uptake (%) and the swelling, S (%) (see details in paragraph below). Considering all the sources of errors associated with our methodology (baseline correction,

178 molar extinction coefficient, thickness of the sample, signal to noise ratio, spectrometer stability), we
179 have evaluated a relative standard uncertainty of about ± 10 % on our results.

180

181 **2.3.2. Data analysis**

182 **2.3.2.1. Polymer swelling**

183 As proposed by Guadagno et al. [20], and shown by Flichy et al. [22] , it is possible to
184 determine polymer swelling using the absorbance of a specific band of polymer before and after
185 exposure to CO_2, according to the Beer-Lambert law:

$$A_0 = \varepsilon . l . C_0 \ \#(1)$$

$$A = \varepsilon . l . C \ \#(2)$$

186 with A_0 and A the absorbances before and after exposure to CO_2; ε the molar extinction coefficient
187 of the polymer band ($L.mol^{-1}.cm^{-1}$); l the sample pathlength (cm); C and C_0 the concentrations of
188 polymer before and after exposure to CO_2 ($mol.L^{-1}$).

189 If V is the volume of the polymer before exposure to gas and $V + \Delta V$ is the volume of the polymer
190 after exposure to the gas, one can write:

$$\frac{C_0}{C} = \frac{V + \Delta V}{V} \ \#(3)$$

$$1 + \frac{\Delta V}{V} = 1 + S \ \#(4)$$

191 By combining these equations (1) to (4), it is possible to determine the swelling (S) with the following
192 Equation (5) [22]:

$$S = \frac{A_0}{A} - 1 \ \#(5)$$

For this study, the broad profile centered at about 4250 cm^{-1} (combination of the C-H stretching and bending modes) have been selected to determine the swelling of both 100 % MAM, at 40 and 130 °C ; PMMA/10 wt% MAM at 40 and 130 °C and PMMA at 130 °C. The integrated absorbance was calculated with a baseline fixed at 4600-3780 cm^{-1}.

For the 100 % PMMA sample at 40 °C, the 4250 cm^{-1} centered profile was close to the saturation. This is why we have used the broad band at about 6000 cm^{-1} (overtone of the C-H stretching modes) with a baseline fixed at 6260-5470 cm^{-1} to determine the integrated absorbance and calculate the polymer swelling. For the other samples, this band centered around 6000 cm^{-1} was unusable due to the too low signal strength.

2.3.2.2. CO_2 sorption

The Beer-Lambert law was applied to the CO_2 peaks in order to determine the concentration of CO_2 sorbed into the polymer. Equation (2) has been adapted to give CO_2 concentration in each polymer and blend in $g.cm^{-3}$:

$$C_{CO_2} = \frac{A}{\varepsilon . l} \times M_{CO_2} \times 10^{-3} \#(6)$$

with A the absorbance of the CO_2 band; ε the molar extinction coefficient of the CO_2 band ($L.mol^{-1}.cm^{-1}$); l the sample pathlentgh (cm) and $M_{CO_2} = 44\ g.mol^{-1}$ the CO_2 molar mass.

In this study, the CO_2 band centered at 4950 cm^{-1} was chosen. In this case, the molar extinction coefficient considered is $\varepsilon_{4950cm^{-1}} = 0.25\ L.mol^{-1}.cm^{-1}$ [11],[21],[31]. The other peaks (2300; 3590; 3695; 4850 and 5030 cm^{-1}) were not used because they were either saturated or too weak and produced large errors linked to the choice of baseline during the determination of both height and integrated area.

The sample thickness was evaluated thanks to spectra of neat CO_2 taken next to the polymer sample in the cell (i.e. on a mirror, orange location represented in Figure 1), at 4 different pressures (Figure 4).

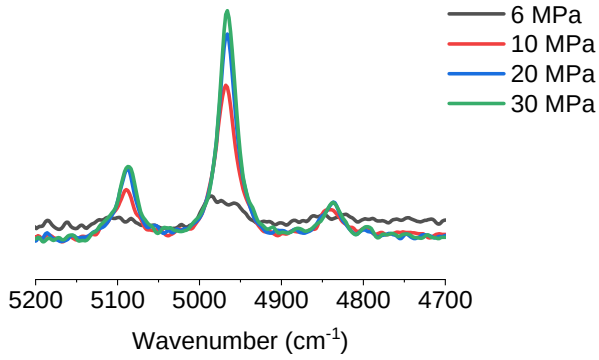

Figure 4: Infrared spectra of CO_2 at T = 40 °C and various pressures ranging from P = 6 MPa (gaseous CO_2) to P = 10-20-30 MPa (supercritical CO_2)

Indeed, by plotting the absorbance (A_{CO_2}) of one of the characteristic peak of CO_2 (4950 cm^{-1} in this study) as a function of CO_2 concentration in the cell (C_{CO_2}), it is possible to determine the pathlength (l) thanks to the following Beer-Lambert equation (Equation (7)). Because C_{CO_2} varies with the saturation pressure and temperature conditions, its value, for each couple of conditions, will be found in the literature tables [32].

$$l = \frac{A_{CO_2}}{\varepsilon \times C_{CO_2}} \#(7)$$

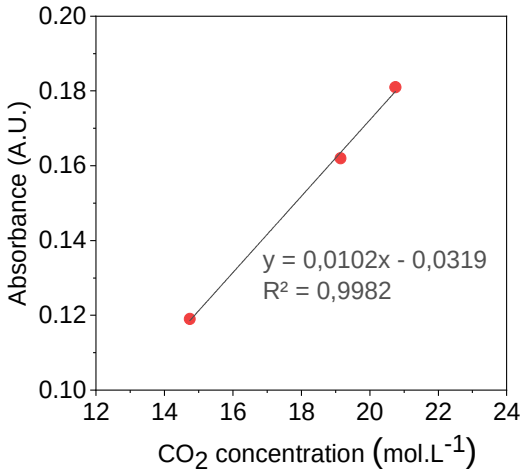

Figure 5: Integrated peak of neat CO_2 absorbance (around 4950 cm^{-1}), as a function of CO_2 concentration in the polymer, at 40 °C (data obtained in the cell out of the sample, during the experiment done with the MAM sample)

As shown in Figure 5, it is possible to determine the pathlength by plotting the absorbance as a function of the CO_2 concentration. Indeed, the slope of the straight line is equal to $\varepsilon.l$ and we know $\varepsilon_{4950cm^{-1}} = 0.25\ L.mol^{-1}.cm^{-1}$. The pathlength thus determined for each samples saturated at (P,T) is representative of the sample thickness. Same procedure was performed for all samples (Figure 3).

Table 3: Samples thicknesses calculated with equation (7)

	l sample at 40 °C (mm)	l sample at 130 °C (mm)
neat PMMA	0.428	0.292
neat MAM	0.408	/
PMMA/10 wt% MAM	0.892	0.38

Finally, the weight percentage of CO_2 (% mass CO_2) sorbed into the polymer was calculated with the following equation:

$$\%\, massCO_2 = \frac{C_{CO_2}}{C_{CO_2} + \frac{\rho_{pol}}{1+S}} \#(8)$$

with $C_{CO_2}$the concentration of CO_2 in the polymer sample (calculated following equation (2)); ρ_{pol} the initial polymer density (g.cm^{-3}) and S the polymer swelling.

3. Results and discussion

3.1. CO_2 sorption through FTIR spectra recovery

The *in situ* CO_2 sorption equilibrium values at 40 °C and 130 °C, for respectively neat PMMA, neat MAM, PMMA/10 wt% MAM blend, at 5 MPa, 10 MPa and 30 MPa, are presented in Figure 6.

A low temperature (40 °C), and pressures up to 30 MPa are typically representative of the conditions that can be used in CO_2 batch foaming for acrylic materials [3]. In the same pressure range, a high temperature (130 °C) is representative of the conditions that can be used in CO_2 extrusion foaming for these kind of PMMA-based materials [24].

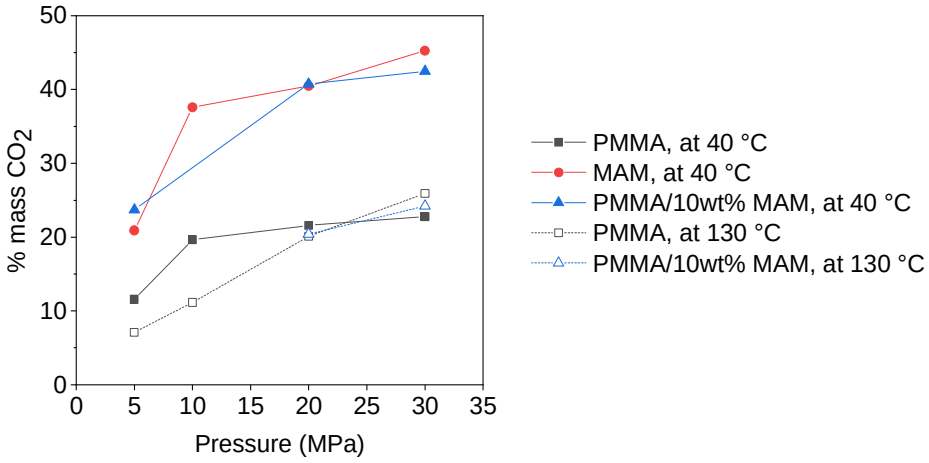

Figure 6: CO_2 mass uptake as function of pressure in PMMA, MAM and PMMA/10 wt% MAM at T = 40 °C and at T = 130 °C

In neat PMMA, the CO_2 concentration in the polymer sample increases with the pressure, no matter the temperature. At 40 °C and 30 MPa the PMMA sample contains 22 wt% CO_2 while at 130 °C and 30 MPa it contains 26 wt% CO_2. These results are quite consistent with values measured by gravimetric methods, as shown in Figure 7 [12],[17].

In neat MAM copolymer at 40 °C, the measured CO_2 sorption values follow the same increasing trend as in PMMA but reaches a much higher value, close to 45 wt% e.g. at 40 °C and 30 MPa. It was impossible to measure the CO_2 sorption at 130°C in MAM using our experimental set-up because of the polymer flow, as previously stated.

Neat MAM or the PMMA/10 wt% MAM blend have a higher CO_2 sorption than neat PMMA in all pressure-temperature conditions because the PBA (central block of the MAM triblock copolymer) have a much higher CO_2 sorption than PMMA (PMMA chains either as homopolymer in the PMMA matrix or as lateral blocks in MAM).

Therefore, the dispersion of MAM as micelles can act as "CO_2-reservoirs" in a PMMA matrix [3][29], and will increase the cell density of our foams. In fact, the 90/10 blend has advantageously a highly nonlinear behavior, i.e. the resulting sorption is not a linear combination of the two polymers sorption. For example, swelling of the PMMA/10 wt% MAM blend may reach values close to those of 100 % MAM at low pressure. Also, the CO_2 sorption of the PMMA matrix is multiplied by 2 as soon as 10 wt% MAM is added.

In the blend (PMMA/10 wt% MAM), at a chosen temperature (40 or 130 °C), the CO_2 mass uptake logically increases with pressure, but in two different trends, one seemingly close to that of neat MAM at 40 °C, and one seemingly close to that of PMMA at 130 °C.

Generally speaking, as observed in various polymers [7],[11],[19], the sorption curves may have different behaviors upon pressure rise. Either the pressure curve is first linear and then it is levelling off (existence of a plateau) or it exhibits a purely linear regime. Indeed Tomasko et al. [7] have shown that depending on the pressure range, the CO_2 sorption is not always proportional to CO_2 pressure. This is due to the variations of the Henry's coefficient (k_H) in Henry's law (Equation 9):

$$C_{CO_2} = k_H \times P_{CO_2} \#(9)$$

with C_{CO_2} the concentration of CO_2 sorbed into the polymer sample (in g.cm^{-3}), k_H the Henry's coefficient (in g.cm^{-3}.MPa^{-1}) and P_{CO_2} the pressure of the CO_2 (in MPa).

Indeed, at low pressure, k_H is often dependent on temperature and polymer state, and at high pressure, k_H may not be constant and becomes dependent on the CO_2 sorption.

In our case, linearity of CO_2 mass uptake (vs pressure) is observed when PMMA/CO_2 mixture is in the rubbery state (130 °C) and therefore a pseudo-Henry's law is obeyed. Even if the intercept is not 0 at 0 MPa, a Henry's coefficient is evaluated from the slope of the $C_{CO_2} = f(P)$ curve (Figure 6). For PMMA at 130°C, k_H = 5.9 10^{-9} Pa^{-1} = 1.4 10^{-5} mol.g^{-1}.bar^{-1}. Our work seems to be the first evaluation of Henry's constant by a FTIR method.

This value is in very good agreement with literature values for other molten polymer/CO_2 solutions. Polymer/CO_2 systems were already studied as C_{CO_2} pressure dependency [33],[34],[35]. Chen at al. [34] found a very similar order of magnitude (6 10^{-9} Pa^{-1}) for melted polypropylene in CO_2, at 200 °C (same pressure range). Rahman et al. [35] found Henry's coefficients between 2 and 5 10^{-5} $mol.g^{-1}.bar^{-1}$ in two melt CO_2-philic diblock copolymers based on poly(ethylene glycol terephthalate) (PEGT) and poly(butylene terephthalate) (PBT), also consistent with our FTIR-determined value of k_H.

On another side, Figure 7, plotting a comparison of CO_2 sorptions in PMMA measured by various methods, shows that FTIR CO_2-sorptions are in good agreement with values obtained following other methods. As an example, in a PMMA/MAM blend at the same (P,T) conditions, Pinto et al. [13] measured a CO_2 uptake of 30 wt% by gravimetry (weighting the sample after batch saturation) at 40 °C and 30 MPa. However, this is a rather low-value, in comparison with our FTIR-measured value of 42 wt%. In our case, we measured the CO_2 sorption in the cell during the saturation whereas they measured it after a possible desorption, once the CO_2 vessel is opened. This difference can principally explain the gap between their value and the one we measured. Another source of difference is the sample geometry and volume.

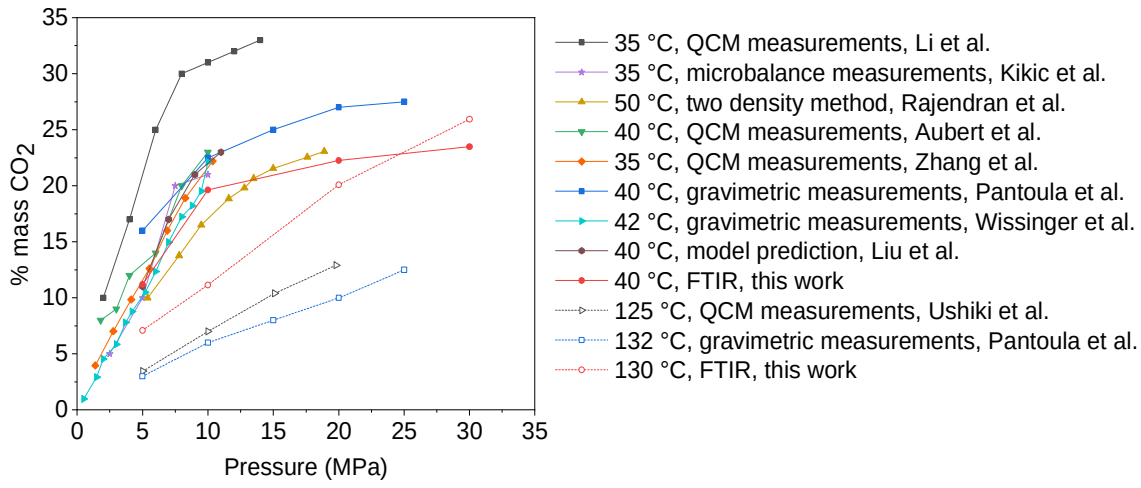

Figure 7 : CO_2 mass uptake in PMMA as a function of pressure, comparison of results obtained following various methods such as quartz crystal microbalance (QCM) [13],[14],[15],[16], microbalance [34], gravimetry [11], two density method (in which both swelling and CO_2-soprtion are simultaneously measured) [17] or FTIR (this work, [35]).

3.2. CO_2 sorption through FTIR spectra recovery

While measuring the *in situ* CO_2 sorption, swelling was evaluated at, respectively, 40 °C and 130 °C under a pressure ranging from 5 to 30 MPa. Swelling of PMMA, MAM and PMMA/10 wt% MAM was calculated with Equation 5, analyzing the polymer peak, and plotted as a function of pressure in Figure 8.Generally speaking, the swelling ratio (S) follows globally a similar trend as solubility with increasing CO_2 pressure.

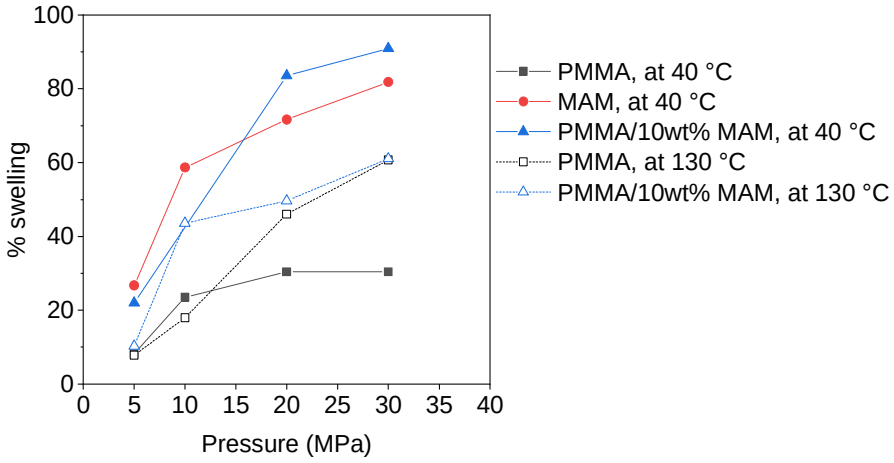

Figure 8 : Percentage of swelling of PMMA, MAM and PMMA/10 wt% MAM blend at 40 °C and 130 °C

For neat PMMA at 40 °C, a swelling plateau value is reached above 20 MPa with a well-defined swelling maximum of roughly 30 %. It shows that the "best" conditions before foaming are attained at a rather low pressure, i.e. there is no need to reach 30 MPa.

The situation is somehow different for PMMA at 130 °C where the state is definitely well above the plasticized T_g of the polymer/CO_2 system, so that the system is able to flow, and swelling is constantly increasing.

In a similar manner, for neat MAM and a blend containing MAM, i.e. a PBA block, no matter the temperature, swelling increases constantly with the pressure and does not reach a plateau value in these conditions. This phenomenon is due to the increase in the free volume where the CO_2 can enter thanks to the mobility of the chains and their disentanglement.

3.3. Correlation between swelling and sorption

In order to evaluate a direct correlation (i.e. a linear proportional relation) between CO_2 solubility and swelling, swelling is plotted as a function of CO_2 mass uptake in Figure 9.

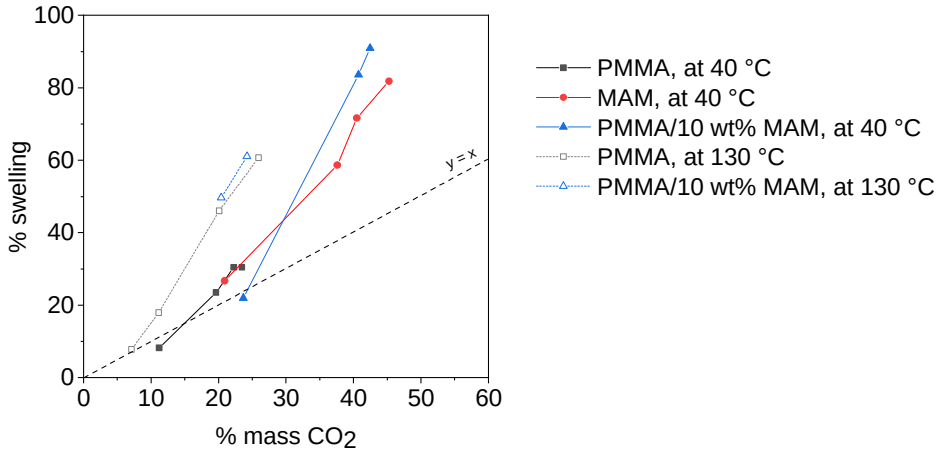

Figure 9: Swelling as a function of CO_2 mass uptake, in PMMA, MAM and PMMA/10 wt% MAM blend

Among studies dealing with several CO_2/amorphous neat polymer homogeneous systems (PS, PMMA, PC,…), studied by any method, a global (not necessarily linear) correlation between swelling and sorption is always observed [18],[36],[37],[38],[39],[40],[41],[42] : a concomitant increase in swelling and sorption in isothermal conditions and a concomitant decrease with temperature in isobaric conditions were observed. Figure 9 also shows this trend in our results.

However, looking at pressure dependencies (e.g. Figure 6, Figure 7, Figure 8) or at swelling-solubility evolution (Figure 9 which is a "pressure-abstracted" dependence), the tendencies are not linear and exhibit several regimes. Figure 7 represents the pressure evolution for several polymers in literature and temperatures, compared to our systems.

and Figure 8 represent only our systems. Plateau pressures, that we name $P^{plateau\ onset}$, were evidenced between 8 to 10 MPa [36] for neat PC at 35 °C; between 8 to 10 MPa for neat PMMA at 33 °C; or between 7 to 8 MPa for neat PMMA at 30 to 35 °C [39]. The plateau is lost above 40 °C, where only linear trends take place for both swelling and mass uptake.

Two regimes observed in the case of pressure dependencies ("isothermal pressure regimes") were defined by Wissinger et al. [36].

Interestingly the two regimes are eligible on all the curves (S = f(P) "dilatation curve", $\%CO_2$ = f(P), "solubility curve", S = f($\%CO_2$) "correlation curve").

Vitoux et al. [19] observed a similar pressure-swelling correlation trend for other non amorphous polymers (hydroxypoly(butadiene), poly(ethylene glycol), polysiloxane). These polymers are either liquid (HPBD, PDMS) or semi crystalline (PEG). Their behavior is the following: upon CO_2 uptake, swelling is first proportional to solubility; then swelling is much "higher" than solubility.

In regime I, isothermal swelling and sorption increase first linearly up to $P^{plateau\ onset}$, above which solublity and swelling level off. Regime I can occur at a temperature ($T^{experiment}$) for which the CO_2/polymer system is (or may become) glassy.

For example, such a case may occur when T_g of polymers (bearing polar functions or atoms) is decreased by the CO_2 interactions [38] leading to a glass transition temperature named T_g^{plasti} (the so called plasticization effect) lower than the experiment saturation temperature.

A plateau regime (regime I) cannot be considered as a true (linear) correlation between sorption and swelling.

In regime II, at a chosen temperature, both sorption and swelling purely linearly increase with the pressure, over a whole pressure range at a given temperature. Such a case may occur in the liquid state of the CO_2/polymer system. These regimes are sketched on Figure 10.

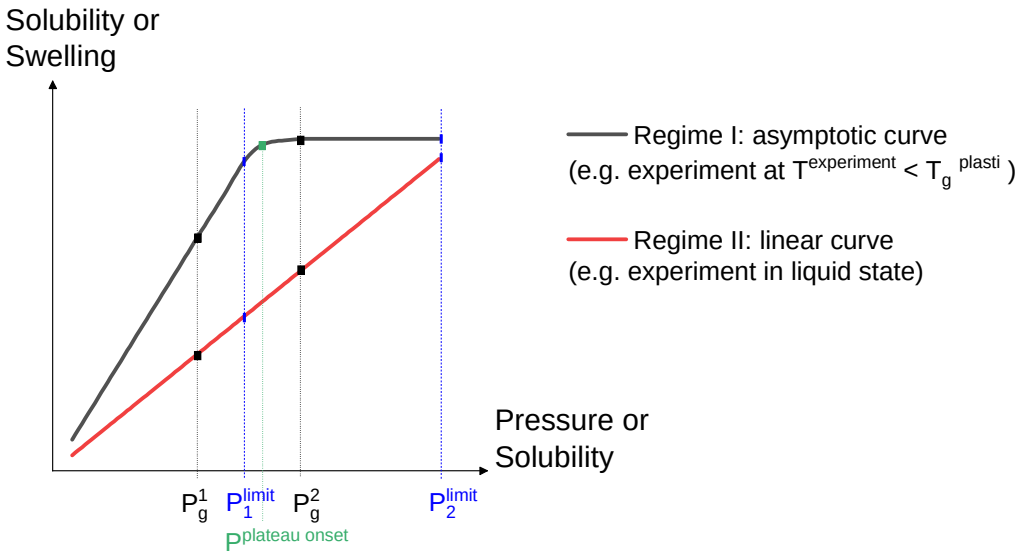

Figure 10: Schematic representation of the two regimes, represented as $\%CO_2$/ S = f(P) or S = f($\%CO_2$); *with two examples of occurrence of regime I or II, and two cases of P_g (P_g^1, P_g^2) and P^{limit} (P^{limit}_1, P^{limit}_2) (here experiments are carried out up to 30 MPa, but often limited to ~ 8-10 MPa in literature)*

The existence of these different regimes is ruled by 4 main inputs: i) the polymer/CO_2 interactions, ii) the capacity of the CO_2 to move through the free volumes and iii) the physical state of a homogeneous or a heterogeneous mixture between polymer and CO_2 [43], iv) the pressure extent that can be investigated and the maximum pressure to which experiments are carried out.

Figure 10 is an attempt to represent schematically the two regimes, plotted as % CO_2/S = f(P) or S = f(% CO_2). In our work, the behavior at 40 °C lies in regime I while behavior at 130 °C lies in regime II.

Most studies found in literature [18],[36],[37],[38],[39],[40],[41],[42] are limited to 10 MPa or less, which does not allow to observe a broad pressure behavior, while our experimental set up allows to go up to 30 MPa (rather high pressure).

We define P^{limit} as the maximum pressure attained for one experiment. Parallelly one can define P_g (called glass transition pressure, P_g), the 'theoretical' transition pressure at which the CO_2/polymer system becomes rubbery (or glassy). Most literature experiments are conducted to a low maximum pressure (e.g. P^{limit} < 5 to 6 MPa) so that P_g pressure is not always attained.

More generally, as far as pressure extent is concerned, two cases arise:

▪ If $P^{limit} < P_g$, the system cannot reach P_g and the free volumes are "saturated or congested" by CO_2. At higher pressure or temperature, enough molecular mobility is triggered and one "gets rid" of free volume effects.

▪ If $P^{limit} > P_g$, one can overcome the CO_2-penetration limit. Upon an isothermal pressure rise, one can increase the penetration of CO_2 (linear regime). Besides, we can make the hypothesis that at still higher pressures (if attainable, but not reached here), the effects of swelling and sorption would counterbalance each other, i.e. the polymer chains would constrain due to isostatic pressure, preventing CO_2 inlet (leading to loss of linearity).

On the contrary, when the system comes to a liquid or liquid-like state, e.g. 130 °C, the regime is linear (CO_2 uptake follows a dissolution mode according to Henry's law). In this regime (type II), there is a true swelling-solubility correlation.

A thermodynamic theoretical analysis is provided by Liu et al. [39] through the calculation and fit of an adjustable interaction parameter (named k_{ij}) and the application of the Sanchez-Lacombe equation of state. They calculated the values of this specific interaction parameter for the CO_2/PMMA solution. They showed its inversely proportional dependency with temperature, and used this only parameter to predict both solubility, swelling and T_g values. Also from their study, P_g is evaluated at ~ 7 MPa (33 °C, 20 wt % CO_2), and P_g ~ 7.5 MPa (42 °C, 18 wt% CO_2).

In comparison to our systems, $P^{plateau\ onset}$ values are estimated from the different swelling and sorption curves, and are reported in Table 4. This table shows the existence of either a plateau pressure or of linearity in the CO_2/polymer systems, coherent with predictions of Liu et al. [39].

On the other side, introducing a heterogeneous component, such as MAM or PBA block in MAM, is probably responsible for deviations from linearity in the swelling-sorption correlation (Figure 9) so that a true correlation cannot be verified.

Table 4: Existence (and pressures values) of either a plateau pressure or linearity in the sorption or swelling curves for the CO_2 systems, PMMA, MAM, PMMA/10 wt% MAM

	Neat PMMA Existence and value of $P^{plateau\ onset}$		**Neat MAM** Existence and value of $P^{plateau\ onset}$		**PMMA/10 wt% MAM** Existence and value of $P^{plateau\ onset}$	
Curve	Sorption=f(P)	Swelling=f(P)	Sorption=f(P)	Swelling=f(P)	Sorption=f(P)	Swelling=f(P)
At 40 °C	Yes at 10 MPa	Yes at 15 MPa	Yes at 10-12 MPa	Yes (poorly defined) at 10-15 MPa	Yes at 8-10 MPa	Yes at 20 MPa
At 130 °C	No	No	/	/	No	No

3.4. Role of heterogeneities

If regimes I or II apply for homogeneous systems, the situation is indeed different when the CO_2 system contains a heterogeneous component, such as PBA in MAM or a MAM/PMMA blend. Here the pressure curves do not exhibit a straight forward behavior of type I or II, e.g. no plateau is well pronounced, or the onset of a plateau is not clear. Consequently, the changes in the pressure curves (swelling or sorption) are revealed as a change of slope or as a slow continuous increase.

More precisely, looking at Figure 9 (plot of swelling VS sorption), the first part of the curve (< 20-25 wt% CO_2) coincides with a good sorption-swelling correlation. In fact, the CO_2-philic component (PBA, MAM) does not attract enough CO_2 to perturbate the correlation; whereas heterogeneities are responsible for perturbation at higher CO_2 solubility (> 20 %).

So in the high CO_2-concentration region (> 25 wt% CO_2), a severe deviation from linearization is obvious. In this region, a true sorption-swelling correlation cannot be possible because of several reasons: different CO_2-philicities, different mobility and dilatation states of phases. Those differences were also previously evidenced by Yang et al. [37] on several poly(alkyl acrylates) and in poly(butyl

457 acrylate) in a pressure scan, especially showing differences in the evolution of void fractions in these
458 polymers.

459 **4. Conclusion**

460 In this paper, the CO_2 uptake (solubility, % CO_2 in polymer) and the polymer swelling (volume change,
461 dilatation) in CO_2 of acrylic systems, namely poly(methyl methacrylate) homopolymer (PMMA), a
462 triblock CO_2-philic rubbery-core acrylic copolymer (MAM) and a PMMA/10 wt% MAM blend has been
463 determined simultaneously using a FTIR microscope combined to a high-pressure cell. Samples were
464 saturated with supercritical CO_2 ($scCO_2$) isothermally at either 40 °C or 130 °C up to high pressures
465 (namely 5 MPa, 10 MPa and 30 MPa), being typical saturation temperatures of a batch $scCO_2$ solid-
466 state foaming or a liquid-like state $scCO_2$ extrusion foaming. Pressures attained in the cell are high
467 compared to previous works.

468 FTIR reveals to be a robust method for *in situ* simultaneous measurement of CO_2 sorption and
469 polymer swelling. The measured values are in very good agreement with data determined by other
470 methods in literature. Besides we provide the first coherent value of a FTIR-determined Henry's
471 coefficient of PMMA in $scCO_2$. Furthermore, the addition of a MAM copolymer at 10 wt% in the
472 PMMA matrix (providing an advantageous heterogeneous system) led to a significant increase of CO_2
473 mass uptake, from 23 % CO_2 for a neat PMMA to 42 % CO_2 for the 10 wt% MAM blend at 40 °C and
474 30 MPa, and of swelling (from 20 % to 90 %). MAM is confirmed as a good additive that enhances
475 PMMA foaming in different processes (solid or liquid-like).

476 If both those CO_2 solubility and polymer swelling are increasing their behavior upon pressure
477 increase is indeed different at the two temperatures in the three systems. We highlighted a purely
478 linear increase or an increase followed by a plateau. Such a behavior corresponds to a specific regime
479 (regime I -asymptotic- or II -linear-, presented schematically on Figure 10). Experimentally we
480 observed either a linear correlation between swelling and sorption or a great deviation from linearity
481 (Figure 9). The existence (or not) of a direct linear correlation is ruled by several inputs: **i)** the

polymer/CO_2 interactions, **ii)** the capacity of the CO_2 to move through the free volumes and to saturate those volumes, **iii)** the physical state of a homogeneous or a heterogeneous mixture between polymer and CO_2 [43], **iv)** the pressure extent that is investigated and the maximum pressure (P^{limit}) to which experiments are carried out.

For example, regime I happens if $P^{limit} < P_g$, the system cannot reach P_g and the free volumes are "saturated or congested" by CO_2 .

On the contrary, when the system comes to a liquid or liquid-like state, e.g. 130 °C, the regime is linear (CO_2 uptake follows a dissolution mode according to Henry's law). In this regime (II), there is a true linear swelling-solubility correlation.

Such data are useful to find out the best routes towards low-density **and** ('and' en gras) nano porous polymer foams, given that the material be should filled with as much as possible CO_2 (at the lower possible pressure). Two chosen temperatures (40 or 130°C) are attempting to mimic a batch or an extrusion process with $scCO_2$ as a foaming agent.

5. Acknowledgments

This work was supported by the French Agence Nationale de la Recherche (ANR) [AAPG PRCE 2018 CE06 0030, 2019]; ANR is gratefully acknowledged.

6. Data availability

The raw/processed data required to reproduce these findings cannot be shared at this time due to time limitations. However, the authors will try to answer questions by e-mails sent to them.

7. References

[1] S. Costeux, H. Jeon, S. Bunker, I. Khan, Nanocellular foams from acrylic polymers: experiments and modeling, in: SPE Foam Conference, Barcelone, 2012.

[2] A. Wagner, A.M. Kreuzer, L. Göpperl, L. Schranzhofer, C. Paulik, Foamable acrylic based ink for the production of light weight parts by inkjet-based 3D printing, European Polymer Journal. 115 (2019) 325–334. https://doi.org/10.1016/j.eurpolymj.2019.03.031.

[3] M. Dumon, J.A.R. Ruiz, J.P. Sanz, M.A.R. Perez, J.-M. Tallon, M. Pedros, E. Cloutet, P. Viot, Block copolymer-assisted microcellular supercritical CO_2 foaming of polymers and blends, Cellular Polymers. 31 (2012) 207–222. https://doi.org/10.1177/026248931203100402.
[4] V. Bernardo, J. Martin-de Leon, J. Pinto, T. Catelani, A. Athanassiou, M.A. Rodriguez-Perez, Low-density PMMA/MAM nanocellular polymers using low MAM contents: Production and characterization, Polymer. 163 (2019) 115–124. https://doi.org/10.1016/j.polymer.2018.12.057.
[5] S. Costeux, D. Foether, Continuous extrusion of nanocellular foams, in: Conference Proceedings Annual Technical Conference-ANTEC, Orlando, 2015: pp. 2740–2745.
[6] E. Kiran, Supercritical fluids and polymers – The year in review – 2014, The Journal of Supercritical Fluids. 110 (2016) 126–153. https://doi.org/10.1016/j.supflu.2015.11.011.
[7] D.L. Tomasko, H. Li, D. Liu, X. Han, M.J. Wingert, L.J. Lee, K.W. Koelling, A review of CO_2 applications in the processing of polymers, Ind. Eng. Chem. Res. 42 (2003) 6431–6456. https://doi.org/10.1021/ie030199z.
[8] C. Okolieocha, D. Raps, K. Subramaniam, V. Altstädt, Microcellular to nanocellular polymer foams: Progress (2004–2015) and future directions – A review, European Polymer Journal. 73 (2015) 500–519. https://doi.org/10.1016/j.eurpolymj.2015.11.001.
[9] M. Haurat, M. Dumon, Amorphous polymers' foaming and blends with organic foaming-aid structured additives in supercritical CO_2 , a way to fabricate porous polymers from macro to nano porosities in batch or continuous processes, Molecules. 25 (2020) 5320. https://doi.org/10.3390/molecules25225320.
[10] J.A. Sarver, E. Kiran, Foaming of polymers with carbon dioxide – The year-in-review – 2019, The Journal of Supercritical Fluids. 173 (2021) 105166. https://doi.org/10.1016/j.supflu.2021.105166.
[11] J. Dubois, E. Grau, T. Tassaing, M. Dumon, On the CO_2 sorption and swelling of elastomers by supercritical CO_2 as studied by in situ high pressure FTIR microscopy, The Journal of Supercritical Fluids. 131 (2018) 150–156. https://doi.org/10.1016/j.supflu.2017.09.003.
[12] M. Pantoula, C. Panayiotou, Sorption and swelling in glassy polymer/carbon dioxide systems Part I. Sorption, The Journal of Supercritical Fluids. 37 (2006) 254–262. https://doi.org/10.1016/j.supflu.2005.11.001.
[13] J. Pinto, J.A. Reglero-Ruiz, M. Dumon, M.A. Rodriguez-Perez, Temperature influence and CO_2 transport in foaming processes of poly(methyl methacrylate)–block copolymer nanocellular and microcellular foams, The Journal of Supercritical Fluids. 94 (2014) 198–205. https://doi.org/10.1016/j.supflu.2014.07.021.
[14] X.-K. Li, G.-P. Cao, L.-H. Chen, R.-H. Zhang, H.-L. Liu, Y.-H. Shi, Study of the anomalous sorption behavior of CO_2 into poly(methyl methacrylate) films in the cicinity of the critical pressure and temperature using a quartz crystal microbalance (QCM), Langmuir. 29 (2013) 14089–14100. https://doi.org/10.1021/la402982b.
[15] J.H. Aubert, Solubility of carbon dioxide in polymers by the quartz crystal microbalance technique, The Journal of Supercritical Fluids. 11 (1998) 163–172. https://doi.org/10.1016/S0896-8446(97)00033-8.
[16] Y. Zhang, K.K. Gangwani, R.M. Lemert, Sorption and swelling of block copolymers in the presence of supercritical fluid carbon dioxide, The Journal of Supercritical Fluids. 11 (1997) 115–134. https://doi.org/10.1016/S0896-8446(97)00031-4.
[17] I. Ushiki, S. Hayashi, S. Kihara, S. Takishima, Solubilities and diffusion coefficients of carbon dioxide and nitrogen in poly(methyl methacrylate) at high temperatures and pressures, The Journal of Supercritical Fluids. 152 (2019) 104565. https://doi.org/10.1016/j.supflu.2019.104565.
[18] A. Rajendran, B. Bonavoglia, N. Forrer, G. Storti, M. Mazzotti, M. Morbidelli, Simultaneous measurement of swelling and sorption in a supercritical CO_2–poly(methyl methacrylate) system, Ind. Eng. Chem. Res. 44 (2005) 2549–2560. https://doi.org/10.1021/ie049523w.

[19] P. Vitoux, T. Tassaing, F. Cansell, S. Marre, C. Aymonier, In situ IR spectroscopy and ab initio calculations to study polymer swelling by supercritical CO_2, J. Phys. Chem. B. 113 (2009) 897–905. https://doi.org/10.1021/jp806709w.
[20] T. Guadagno, S.G. Kazarian, High-pressure CO_2 -expanded solvents: simultaneous measurement of CO_2 sorption and swelling of liquid polymers with in-situ sear-IR spectroscopy, J. Phys. Chem. B. 108 (2004) 13995–13999. https://doi.org/10.1021/jp0481097.
[21] M. Champeau, J.-M. Thomassin, C. Jérôme, T. Tassaing, In situ FTIR micro-spectroscopy to investigate polymeric fibers under supercritical carbon dioxide: CO2 sorption and swelling measurements, The Journal of Supercritical Fluids. 90 (2014) 44–52. https://doi.org/10.1016/j.supflu.2014.03.006.
[22] N.M.B. Flichy, S.G. Kazarian, C.J. Lawrence, B.J. Briscoe, An ATR−IR study of poly (dimethylsiloxane) under high-pressure carbon dioxide: simultaneous measurement of sorption and swelling, J. Phys. Chem. B. 106 (2002) 754–759. https://doi.org/10.1021/jp012597q.
[23] M.D. Elkovitch, L.J. Lee, D.L. Tomasko, Effect of supercritical carbon dioxide on PMMA/rubber and polystyrene/rubber blending: Visosity ratio and phase inversion, Polym. Eng. Sci. 41 (2001) 2108–2125. https://doi.org/10.1002/pen.10906.
[24] S. Siripurapu, Y.J. Gay, J.R. Royer, J.M. DeSimone, J. Spontak, S.A. Khan, Generation of microcellular foams of PVDF and its blends using supercritical carbon dioxide in a continuous process, (2002) 10.
[25] B. Notario, J. Pinto, E. Solorzano, J.A. de Saja, M. Dumon, M.A. Rodríguez-Pérez, Experimental validation of the Knudsen effect in nanocellular polymeric foams, Polymer. 56 (2015) 57–67. https://doi.org/10.1016/j.polymer.2014.10.006.
[26] T. Li, G. Zhao, G. Wang, L. Zhang, J. Hou, Thermal-insulation, electrical, and mechanical properties of highly-expanded PMMA/MWCNT nanocomposite foams fabricated by supercritical CO_2 foaming, Macromol. Mater. Eng. 304 (2019) 1800789. https://doi.org/10.1002/mame.201800789.
[27] L. Lalande, C.J.G. Plummer, J.-A.E. Månson, P. Gérard, Microdeformation mechanisms in rubber toughened PMMA and PMMA-based copolymers, Engineering Fracture Mechanics. 73 (2006) 2413–2426. https://doi.org/10.1016/j.engfracmech.2006.05.014.
[28] J.A.R. Ruiz, M. Pedros, J.-M. Tallon, M. Dumon, Micro and nano cellular amorphous polymers (PMMA, PS) in supercritical CO_2 assisted by nanostructured CO_2-philic block copolymers – One step foaming process, The Journal of Supercritical Fluids. 58 (2011) 168–176. https://doi.org/10.1016/j.supflu.2011.04.022.
[29] J. Pinto, M. Dumon, M. Pedros, J. Reglero, M.A. Rodriguez-Perez, Nanocellular CO_2 foaming of PMMA assisted by block copolymer nanostructuration, Chemical Engineering Journal. 243 (2014) 428–435. https://doi.org/10.1016/j.cej.2014.01.021.
[30] V. Bernardo, J. Martin-de Leon, E. Laguna-Gutierrez, T. Catelani, J. Pinto, A. Athanassiou, M.A. Rodriguez-Perez, Understanding the role of MAM molecular weight in the production of PMMA/MAM nanocellular polymers, Polymer. 153 (2018) 262–270. https://doi.org/10.1016/j.polymer.2018.08.022.
[31] S. Foltran, E. Cloutet, H. Cramail, T. Tassaing, In situ FTIR investigation of the solubility and swelling of model epoxides in supercritical CO_2, The Journal of Supercritical Fluids. 63 (2012) 52–58. https://doi.org/10.1016/j.supflu.2011.12.015.
[32] NIST: https://webbook.nist.gov/chemistry/, n.d.
[33] K.-H.J. Chen, S.S.H. Rizvi, Measurement and prediction of solubilities and diffusion coefficients of carbon dioxide in starch-water mixtures at elevated pressures, J. Polym. Sci. B Polym. Phys. 44 (2006) 607–621. https://doi.org/10.1002/polb.20703.
[34] J. Chen, T. Liu, W. Yuan, L. Zhao, Solubility and diffusivity of CO_2 in polypropylene/micro-calcium carbonate composites, The Journal of Supercritical Fluids. 77 (2013) 33–43. https://doi.org/10.1016/j.supflu.2013.02.007.

[35] Md.M. Rahman, J. Lillepärg, S. Neumann, S. Shishatskiy, V. Abetz, A thermodynamic study of CO_2 sorption and thermal transition of PolyActive™ under elevated pressure, Polymer. 93 (2016) 132–141. https://doi.org/10.1016/j.polymer.2016.04.024.
[36] R.G. Wissinger, M.E. Paulaitis, Swelling and sorption in polymer–CO_2 mixtures at elevated pressures, J. Polym. Sci. B Polym. Phys. 25 (1987) 2497–2510. https://doi.org/10.1002/polb.1987.090251206.
[37] Y. Yang, A.K. Narayanan Nair, S. Sun, Sorption and diffusion of methane and carbon dioxide in amorphous poly(alkyl acrylates): A molecular simulation study, J. Phys. Chem. B. 124 (2020) 1301–1310. https://doi.org/10.1021/acs.jpcb.9b11840.
[38] S.G. Kazarian, M.F. Vincent, F.V. Bright, C.L. Liotta, C.A. Eckert, Specific intermolecular interaction of carbon dioxide with polymers, J. Am. Chem. Soc. 118 (1996) 1729–1736. https://doi.org/10.1021/ja950416q.
[39] D. Liu, H. Li, M.S. Noon, D.L. Tomasko, CO_2 -Induced PMMA swelling and multiple thermodynamic property analysis using Sanchez−Lacombe EOS, Macromolecules. 38 (2005) 4416–4424. https://doi.org/10.1021/ma047319e.
[40] T.M. Fieback, F. Dreisbach, New approach for simultaneous measurement of gas absorption and swelling, Ind. Eng. Chem. Res. 50 (2011) 7049–7055. https://doi.org/10.1021/ie200076k.
[41] M.Z. Hossain, A.S. Teja, Correlation/prediction of sorption, swelling, and cloud points in CO_2 + polymer systems, The Journal of Supercritical Fluids. 122 (2017) 58–62. https://doi.org/10.1016/j.supflu.2016.12.003.
[42] C. Tsioptsias, C. Panayiotou, Simultaneous determination of sorption, heat of sorption, diffusion coefficient and glass transition depression in polymer–CO_2 systems, Thermochimica Acta. 521 (2011) 98–106. https://doi.org/10.1016/j.tca.2011.04.011.
[43] Y. Dong Hwang, S. Woon Cha, The relationship between gas absorption and the glass transition temperature in a batch microcellular foaming process, Polymer Testing. 21 (2002) 269–275. https://doi.org/10.1016/S0142-9418(01)00081-2.

Table 5: Raw data recorded in FTIR for neat PMMA (d = 1.19); neat MAM (d = 1.03) and PMMA/10 wt% MAM (d = 1.18) at 40 °C and 130 °C varying the baselines for the peak absorbance measurement and mean data calculated.

PMMA at 40°C

Baseline (6290.785-5496.217 cm^{-1})		
Pressure (MPa)	Absorbance	Swelling (%)
0.10	74.39	0
5	68.37	8.79
10	60.45	23.05
20	56.59	31.44
30	56.60	31.41
Baseline (6311.971-5496.217 cm^{-1})		
Pressure (MPa)	Absorbance	Swelling (%)
0.10	72.01	0
5	68.10	5.74
10	58.15	23.85
20	55.53	29.67
30	55.93	28.76
Baseline (6473.965-5496.217 cm^{-1})		
Pressure (MPa)	Absorbance	Swelling (%)
0.10	73.72	0
5	66.99	10.05
10	59.63	23.62
20	56.64	30.15
30	56.24	31.08

Mean				
Pressure (MPa)	Swelling (%)	Swelling	C_{CO_2} ($g.cm^{-3}$)	% mass CO_2
5	8.20	0.08	0.14	11.21
10	23.51	0.24	0.24	19.63
20	30.42	0.30	0.26	22.25
30	30.41	0.30	0.28	23.48

PMMA at 130°C

Baseline (4607.180-3787.569 cm^{-1})		
Pressure (MPa)	Absorbance	Swelling (%)
0.10	241.41	0
5	224.85	7.37
10	203.91	18.39
20	166.08	45.36
30	152.45	58.35
Baseline (4784.602-3787.569 cm^{-1})		
Pressure (MPa)	Absorbance	Swelling (%)
0.10	246.39	0
5	229.67	7.28
10	209.99	17.33
20	170.00	44.93
30	155.06	58.90
Baseline (4761.459-3770.212 cm^{-1})		
Pressure (MPa)	Absorbance	Swelling (%)
0.10	234.22	0
5	215.55	8.66
10	198.23	18.15
20	158.49	47.78
30	142.04	64.89

Mean				
Pressure (MPa)	Swelling (%)	Swelling	C_{CO_2} ($g.cm^{-3}$)	% mass CO_2
5	8.01	0.08	0.08	7.10
10	18.27	0.18	0.13	11.15
20	46.57	0.47	0.20	20.09
30	61.62	0.62	0.26	25.93

MAM at 40°C

Baseline (4607.180-3810.710 cm^{-1})		
Pressure (MPa)	Absorbance	Swelling (%)
0.10	221.56	0
5	171.37	29.29
10	138.93	59.48
20	128.50	72.42
30	121.75	81.99
Baseline (4643.821-3804.925 cm^{-1})		
Pressure (MPa)	Absorbance	Swelling (%)
0.10	202.17	0
5	162.35	24.52
10	128.82	56.94
20	119.41	69.31
30	111.81	80.82
Baseline (4576.324-3804.925 cm^{-1})		
Pressure (MPa)	Absorbance	Swelling (%)
0.10	211.15	0
5	167.10	26.37
10	132.24	59.67
20	121.83	73.31
30	115.54	82.75

Mean				
Pressure (MPa)	Swelling (%)	Swelling	C_{CO_2} ($g.cm^{-3}$)	% mass CO_2
5	26.73	0.27	0.22	20.97
10	58.70	0.59	0.39	37.69
20	71.68	0.72	0.41	40.58
30	81.85	0.82	0.47	45.36

PMMA/10 wt% MAM (M53) at 40°C

Baseline (4607.180-3837.709 cm^{-1})		
Pressure (MPa)	Absorbance	Swelling (%)
0.10	442.08	0
5	364.42	21.31
10	-	-
20	243.68	81.42
30	235.39	87.81
Baseline (4763.388-3855.066 cm^{-1})		
Pressure (MPa)	Absorbance	Swelling (%)
0.10	448.39	0
5	374.64	19.69
10	-	-
20	251.48	78.30
30	244.17	83.64
Baseline (4607.180-3806.854 cm^{-1})		
Pressure (MPa)	Absorbance	Swelling (%)
0.10	458.06	0
5	366.49	24.99
10	-	-
20	239.85	90.98
30	227.52	101.32

Mean				
Pressure (MPa)	Swelling (%)	Swelling	C_{CO_2} ($g.cm^{-3}$)	% mass CO_2
5	21.99	0.22	0.30	23.39
10	-	-	-	-
20	83.59	0.84	0.39	37.61
30	90.92	0.91	0.40	39.28

692 **PMMA/10 wt% MAM (M53) at 130°C**

Baseline (4607.180-3787.569 cm^{-1})		
Pressure (MPa)	Absorbance	Swelling (%)
0.10	315.01	0
5	280.55	12.31
10	216.25	45.71
20	210.20	49.91
30	195.07	61.53
Baseline (4767.245-3787.569 cm^{-1})		
Pressure (MPa)	Absorbance	Swelling (%)
0.10	319.19	0
5	292.09	9.28
10	-	-
20	214.86	48.55
30	200.00	59.60
Baseline (4990.951-3787.569 cm^{-1})		
Pressure (MPa)	Absorbance	Swelling (%)
0.10	32..59	0
5	295.55	9.15
10	228.08	41.44
20	214.40	50.47
30	199.07	62.05

Mean				
Pressure (MPa)	Swelling (%)	Swelling	C_{CO_2} ($g.cm^{-3}$)	% mass CO_2
5	10.25	0.10		
10	43.57	0.44		
20	49.64	0.50	0.2	20.54
30	61.06	0.61	0.24	24.38

693